NEOPLASIA
www.neoplasia.com

Volume 10 Number 2 February 2008 pp. 149–159 149

The Role of Fascin in the Migration and Invasiveness of Malignant Glioma Cells[1]

Jeong Hyun Hwang*,†, Christian A. Smith†, Bodour Salhia‡ and James T. Rutka†

*Department of Neurosurgery, School of Medicine, Kyungpook National University, Daegu, South Korea; †The Arthur and Sonia Labatt Brain Tumor Research Center, The Hospital for Sick Children, The University of Toronto, Toronto, Ontario, Canada; ‡The Translational Genomics Research Institute, Phoenix, AZ, USA

Abstract

Malignant glioma is the most common primary brain tumor, and its ability to invade the surrounding brain parenchyma is a leading cause of tumor recurrence and treatment failure. Whereas the molecular mechanisms of glioma invasion are incompletely understood, there is growing evidence that cytoskeletal–matrix interactions contribute to this process. Fascin, an actin-bundling protein, induces parallel actin bundles in cell protrusions and increases cell motility in multiple human malignancies. The role of fascin in glioma invasion remains unclear. We demonstrate that fascin is expressed in a panel of human malignant glioma cell lines, and downregulation of fascin expression in glioma cell lines by small interfering RNA (siRNA) is associated with decreased cellular attachment to extracellular matrix (ECM) and reduced migration. Using immunofluorescence analysis, we show that fascin depletion results in a reduced number of filopodia as well as altered glioma cell shape. *In vitro* invasiveness of U251, U87, and SNB19 glioma cells was inhibited by fascin siRNA treatment by 52.2%, 40.3%, and 23.8% respectively. Finally, we show a decreased invasiveness of U251-GFP cells by fascin knockdown in an *ex vivo* rat brain slice model system. This is the first study to demonstrate a role for fascin in glioma cell morphology, motility, and invasiveness.

Neoplasia (2008) 10, 149–159

Introduction

Malignant gliomas are the most common primary brain tumors [1]. Currently, surgery and radiation therapy followed by treatment with temozolomide is the treatment protocol of choice for patients with glioblastoma multiforme [2,3]. However, despite advanced multimodal treatment, the median life expectancy for patients with glioblastoma multiforme is approximately 14 months with less than 5% of patients alive at 5 years after diagnosis [4,5]. Although systemic metastases of malignant gliomas are relatively rare, the highly infiltrative nature of glioma cells that invade into surrounding brain parenchyma is a major cause of treatment failure and tumor recurrence [6,7]. Glioma invasion is a multifactorial process consisting of glioma cell interactions with normal cellular constituents such as astrocytes, neurons, and endothelial cells, interactions with the extracellular matrix (ECM), proteolysis of ECM components, and migration [8].

To migrate, glioma cells must modify their shape and rigidity to interact with the surrounding environment [9]. Typically, a migrating glioma cell will remodel its cytoskeleton to form cellular protrusions and focal adhesions at the leading edge, and generate tensile forces to move the cell body forward. Cellular protrusions known as filopodia are considered essential processes in cell migration because they function as sensors of the external microenvironment and as plasma membrane extensions that form initial contacts with the ECM. The rearrangement of actin microfilaments into strong parallel actin bundles within or near filopodia is a key component of the migration

Address all correspondence to: James T. Rutka, MD, PhD, Division of Neurosurgery, Suite 1503, The Hospital for Sick Children, 555 University Avenue, Toronto, Ontario, Canada M5G 1X8. E-mail: james.rutka@sickkids.ca

[1]This work was supported by a grant from the Canadian Institutes of Health Research (CIHR; MOP-74610) and was supported by Brainchild, the Wiley Fund, and the Laurie Berman Fund for Brain Tumor Research. J. T. Rutka was supported as a Scientist of the CIHR. B. Salhia was supported by a Restracomp fellowship from The Hospital for Sick Children and by a Canada Graduate Scholarship Award from the CIHR.
Received 11 October 2007; Revised 28 November 2007; Accepted 28 November 2007

DOI 10.1593/neo.07909

process [10–13]. Reorganization of the actin microfilamentous system has previously been associated with alterations in glioma morphology and invasiveness [14].

Several actin-binding proteins have been described including α-actinin, tropomyosin, fimbrin, villin, and fascin [11]. Fascin is a key actin-bundling protein that provides rigidity to filopodial bundles [13,15]. Fascin was first isolated from sea urchin egg extracts [16], and then identified in *Drosophila* [17] and in human B-lymphocytes [18]. Fascin has been shown to be expressed at high levels in the brain, ovary, and testis [19]. In the brain, fascin expression has been localized to neurons, glial cells, and endothelial cells [19–22]. Fascin colocalizes with filopodia, microspikes, lamellopodia, and stress fibers [20,23]. Additionally, fascin has been shown to localize to lamellipodia and filopodia in growth cones of cultured neurons [12,18]. These findings suggest that fascin may play an important role in the formation of actin-based structures, such as filopodia and lamellipodia, and in the migratory behavior of cells.

Fascin expression is increased in different types of cancers including breast, lung, ovary, esophagus, kidney, and colon [24–33]. In addition, high fascin expression has been observed in many transformed cells and carcinoma cell lines [15,24,26,29,34]. Cancer cells expressing high levels of fascin exhibit morphologic characteristics, such as increased membrane protrusions and migration ability. However, little is known about the role of fascin in human brain tumors. Recently, two studies reported the relationship between fascin expression and human gliomas [35,36]. Both studies demonstrate that an increase in fascin expression is associated with increasing tumor grade in glial tumors. To date, no studies have examined the consequences of fascin manipulations in experimental glioma cell systems. Accordingly, to determine if fascin plays a role in the migratory capacity of glioma cells, we have used small interfering RNAs (siRNA) to suppress the expression of fascin in glioma cells. Here we report our results on fascin knockdown on glioma cell proliferation, adhesion, migration, and invasivenevess *in vitro* and in an *ex vivo* rat brain slice model system.

Material and Methods

Cell Culture and Extracellular Matrix

The permanent, well-characterized human glioma cell lines U251, U87, SNB19, U138, T98, and U118 were received from the American Type Culture Collection (Manassas, VA). The U343 cell line was obtained from Brain Tumor Research Center, University of California (San Francisco, CA). U251-GFP, a glioma cell line stably expressing green fluorescence protein (GFP), was provided by Michael Berens (The Translational Genomics Research Institute, Phoenix, AZ). Glioma cells were maintained in Dulbecco's modified Eagle's medium (DMEM) supplemented with 10% fetal bovine serum (FBS) and cultured at 37°C, 5% CO_2 in a humidified chamber. Normal human astrocytes were purchased from Clonetics (East Rutherford, NJ) and maintained in ABM media containing 3% FBS, 0.1% ascorbic acid, 0.5% recombinant human epidermal growth factor, 0.1% GA-1000, 0.25% insulin, and 1% l-glutamine (all from Clonetics). The human ECM proteins laminin, vitronectin, fibronectin, and collagen type IV were obtained from Sigma (St. Louis, MO).

Small Interfering RNA Preparation and Transfections

Small interfering RNA (siRNA) duplexes specific for Fascin1 were designed according to Elbashir et al. [37]. Two different Fascin siRNA sequences were used: Fs1, corresponding to 113 to 133 bp after the start codon of the *Fascin1* gene (5′ GCAGCCTGAAGAAGAAGCA), and Fs2, corresponding to 1340 to 1360 bp after the start codon of the *Fascin1* gene (5′ CTCCTGTGGACTTCTTCTTTT). The 21-nt RNA was purchased from Eurogentec (San Diego, CA) in deprotected and desalted forms. As a control for off-target effects caused by RNA interference, nontargeting siRNA, designed to have at least four mismatches to any human and mouse species, was used (Dharmacon, Lafayette, CO). Transient transfections of siRNA (50 nM final concentration) against Fascin1 were carried out using Lipofectamine 2000 (Invitrogen, Carlsbad, CA). Cells were plated at 60% confluency in DMEM containing 10% serum without antibiotics and transfections were carried out 24 hours later. Lipofectamine 2000 was diluted in serum-free DMEM for 5 minutes and the siRNA was diluted in serum-free DMEM. The two mixtures were combined and incubated for 20 minutes at room temperature to enable transfection complex formation. The complexes were subsequently added to the cells. Transfections with Lipofectamine 2000 alone served as controls. Maximal depletion was achieved by day 3 after transfection, and cells were assayed at 72 hours after transfection. Fascin expression was determined by western blot analysis using an anti–human fascin monoclonal antibody (1:1000; DakoCytomation, Carpinteria, CA).

Western Blot Analysis

Total cell lysates were prepared in a lysis buffer (50 mM Tris pH 7.4, 1% Triton X-100, 2 mM EDTA, 150 mM NaCl) with a cocktail of protease inhibitors (Roche Diagnostics, Basel, Switzerland). Lysates were cleared by centrifugation and mixed with SDS sample buffer containing Tris pH 6.8, 2% SDS, glycerol and β-mercaptoethanol. The protein concentration was estimated by Lowry method using DC Protein Assay Kit (Bio-Rad, Hercules, CA) and 10 μg of protein extracts were separated by SDS-PAGE, and transferred to polyvinyldifluoride membranes (Millipore, Bedford, MA). The membranes were subsequently blocked with 5% skim milk in TBS–T (50 mM Tris pH 7.5, 150 mM NaCl, and 0.1% Tween 20) for 1 hour at room temperature and incubated overnight at 4°C with the primary antibodies described above. A monoclonal antibody against the human transferrin receptor (1:1000; Zymed, South San Francisco, CA) was used on the same blot and served as a loading control. The membranes were subsequently incubated at room temperature for 1 hour with horseradish peroxidase–linked goat anti–mouse IgG (Bio-Rad, Hercules, CA) and analyzed using Western Blotting Luminol Reagent (PerkinElmer Life Sciences, Boston, MA).

Cell Viability Assay

Cell viability was determined using the colorimetric MTS assay. Cells transiently transfected with two different siRNA oligonucleotides were trypsinized, counted and resuspended in DMEM with 10% FBS at 6 hours after transfection. The cells were plated in 96-well dishes at a density of 5000 cells/well and were allowed to adhere overnight. Cells were transfected with Lipofectamine 2000–complexed fascin siRNA or nontargeting siRNA. Cells were tested in quadruplicate with MTS [3-(4,5-dimethylthiazol-2-yl)-5-(3-carboxymethoxyphenyl)-2-(4-sulfophenyl)-2*H*-tetrazolium, inner salt (Promega, Madison, WI)] to assess cell viability at 24 and 72 hours after transfection. The MTS assay was performed according to the manufacturer's instructions. MTS coupled with an electron-coupling reagent (phenazine ethosulfate) was added to each well of cells and

incubated at 37°C in a humidified chamber for 1 hour. Absorbance of the reaction was measured at 490 nm using a microtiter plate reader (VersaMax; Molecular Devices Corp., Sunnyvale, CA). The quantity of formazan product, as measured by absorbance, is directly proportional to the number of living cells. Absorbance was plotted as a percentage of the control value. All experiments were repeated in triplicate and repeated three independent times.

Cell Attachment Assay

The cell attachment assay was performed as described previously [37,38] with modifications. Ninety-six–well plates were incubated at 4°C overnight with different ECM proteins (laminin and fibronectin at 10 μg/ml, collagen type IV at 50 μg/ml, and vitronectin at 1 μg/ml). The unbound sites were blocked with 0.1% BSA in PBS for 1 hour at 37°C. Control dishes were prepared by blocking with BSA alone. Glioma cells were detached, resuspended in serum-free medium at 72 hours after transfection, then plated at 5×10^4 cells/well on ECM protein- or BSA-coated plates. The cells were allowed to adhere for 3 hours at 37°C and 5% CO_2 in a humidified chamber. Unattached cells were removed by washing with PBS three times, and the remaining cells were fixed with 4% paraformaldehyde and stained with 0.5% crystal violet. The excess stain was washed away with water then air-dried overnight. The crystal violet bound to the attached cells was solubilized with 1% SDS and the absorbance of each well was measured at 595 nm using a microtiter plate reader (Molecular Devices Corp.). All experiments were repeated three times with five replicates.

Cell Migration Assay

Cell migration assays were performed using the microliter-scale radial monolayer assay as described previously [6,14,39,40]. Briefly, 10-well Teflon-coated slides (CSM Inc., Phoenix, AZ) were coated with different ECM proteins and 0.1% BSA as described above. Cells transfected with siRNA for Fascin1 or nontargeting oligonucleotide were collected 24 hours after transfection and seeded through a cell sedimentation manifold (CSM Inc.) at 3000 cells/well to establish a circular confluent monolayer, 1 mm in diameter, at the center of the substrate-coated well. Photographs were taken 16 hours after plating and a circle of best-fit circumscribing the cells was drawn. The cells were allowed to migrate for a 24-hour period, and another circle circumscribing the newly migrated cells was made. The average migration rate was calculated as the change in the diameter of the circle circumscribing the cell population over a 24-hour period (micrometers per 24 hours). Photomicrographs were taken with an inverted microscope (Leica DM IRE2; Leica Microsystems, Bannokburn, IL) and analyzed using image analysis software (Scion Image, Frederick, MD). All experiments were repeated in five replicates and experiments were repeated three times.

Cell Invasion Assay

A cell invasion assay was carried out using modified Boyden Chambers consisting of Transwell-precoated Matrigel membrane filter inserts with 8 μm pores in 24-well tissue culture plates (BD Biosciences, Bedford, MA) as described previously [40]. Two days after transfection with siRNA, 4×10^4 cells were plating onto the top of the chamber in DMEM with 5% FBS and the bottom chamber was filled with DMEM containing 20% FBS as a chemoattractant. After 24 hours of incubation in a 5% CO_2 humidified chamber at 37°C, noninvading cells were removed by wiping the upper surface of the membrane with a cotton swab, and the filter membrane was fixed with 4% paraformaldehyde and stained with 0.5% crystal violet. The degree of invasion was quantified by counting the cells that had migrated through the membrane in at least six random fields (total magnification, ×200) per filter. Experiments were repeated three times in triplicate.

Ex Vivo *Brain Slice Invasion Assay*

The *ex vivo* rat brain slice model system was modified from the organotypic culture methods reported previously [40–43]. Briefly, the brain tissue was prepared from 4-week-old male Wistar rats (Charles River Laboratories Inc., Wilmington, MA). After administration of isoflurane anesthesia, the cerebrum was removed and cut vertically to the base in 400-μm sections using a tissue slicer (EMS 4000; Electron Microscopy Science, Hatfield, PA). The brain slices were transferred to the upper chamber of a transwell insert and placed on top of the 0.4-μm micropore polycarbonate filter (BD Biosciences) in a six-well tissue culture plate. The brain slices were incubated at least 24 hours before cell seeding at 37°C and 5% CO_2 in a humidified chamber in DMEM with 10% FBS, 100 U/ml penicillin, 100 μg/ml streptomycin, and 2.5 μg/ml amphotericin B. Three days after transfection with siRNA, U251-GFP cells were trypsinized and resuspended in serum-free medium to 2×10^8 cells/ml, and 10^5 glioma cells (0.5 μl transfer volume) were placed on the center of the putamen. The cells were allowed to invade into the brain slice for 72 hours. Six brain slices were used in each experiment. To quantitate glioma cell invasion, the brain slice was fixed overnight in 4% paraformaldehyde at 4°C, and fluorescent imaging was taken at 10× magnification using an inverted laser confocal microscope (LSM 510 META; Carl Zeiss Inc., Thronwood, NY). To assess the depth of invasion in control and fascin siRNA–transfected cell populations, serial sections were obtained every 10 μm downward from the top surface to the bottom of the slice after 72 hours. The LSM 510 software (Carl Zeiss Inc.) was used to calculate the total area of GFP-stained cells in each section and the extent of glioma cell invasion was defined as the depth of penetration (in μm) after 72 hours to which the invading cells penetrated the brain slice as described previously [40]. The animal protocol described here was approved by the Institutional Animal Care Committee. All experiments were repeated three times.

Immunofluorescence and Confocal Microscopy

Cells transfected by siRNA were plated onto coverslips precoated with laminin (10 μg/ml) 24 hours after transfection. At 72 hours after transfection, cells were washed three times with PBS and fixed with 4% paraformaldehyde for 10 minutes and permeabilized for 5 minutes with 0.5% Triton X-100 in PBS at room temperature. Nonspecific binding was blocked by 1% BSA in PBS for 1 hour at room temperature. Subsequently, cells were incubated with an anti–fascin monoclonal antibody (1:200; DakoCytomation) for 1 hour. After washing, cells were then incubated with Alexa Fluor 488– (Molecular Probes, Eugene, OR) conjugated goat anti–mouse IgG secondary antibodies for 30 minutes at room temperature. For double labeling with F-actin, cells were coincubated with Texas Red-X phalloidin (1:50 dilution; Molecular Probes). A Zeiss Axiovert 200M Spinning Disk confocal microscope (Carl Zeiss Inc.) installed with a Hamamatsu Back-Thinned EM-CCD camera (Hamamatsu, Bridgewater, NJ) was used to visualize fluorescence.

Statistical Analyses

Data are expressed as mean ± standard error (SE). Statistical analyses were performed with Student's *t* test and Mann-Whitney *U* test. A *P* value of < .05 was considered statistically significant.

Results

Fascin Expression in Glioma Cell Lines and Fascin Silencing by siRNA Transfection

Western blot analysis was performed on all the different glioma cell lines including U138, T98, U251, U87, SNB19, U343, and U118 as well as normal human astrocytes. All glioma cells tested and normal human astrocytes showed fascin expression (Figure 1*A*). Of the cell glioma cell lines examined, we selected three, U251, U87, and SNB19, for further study as they were comparable in terms of fascin expression levels and were well characterized previously in terms of *in vitro* growth kinetics.

Fascin knockdown was achieved following transient transfection with two different fascin siRNA duplexes (Figure 1*B*). In all experiments, a nontargeting oligonucleotide was used to exclude nonspecific off-target effects of RNA interference. Fascin knockdown was observed following 24 hours after siRNA transfection, and reached maximum depletion at 72 hours after transfection (Figure 1*C*). Therefore, subsequent experiments such as adhesion, migration, invasion, and immunofluorescent studies were performed 72 hours after transfection to analyze the functional effects of fascin depletion.

Fascin Downregulation and Glioma Cell Viability

An MTS cell viability assay was used to examine the effects of fascin knockdown on glioma cells. At 72 hours after transfection, cell viability was unaffected in U251 and SNB19 glioma cells, and minimally affected in U87 cells (13% decrease in cell viability compared to untransfected and nontargeting siRNA controls) (data not shown).

Fascin Knockdown Reduces Filopodia Formation in Glioma Cells

Immunofluorescence was used to examine the effects of fascin knockdown on cell morphology. Cells were seeded on laminin-coated coverslips given that previous studies have shown laminin to be the most permissive ECM substrate for glioma cell motility [6,44]. Fascin localized to the perinuclear cytoplasm and actin-rich membrane ruffles at the leading edge (Figure 2). SNB19 and U251 cells showed

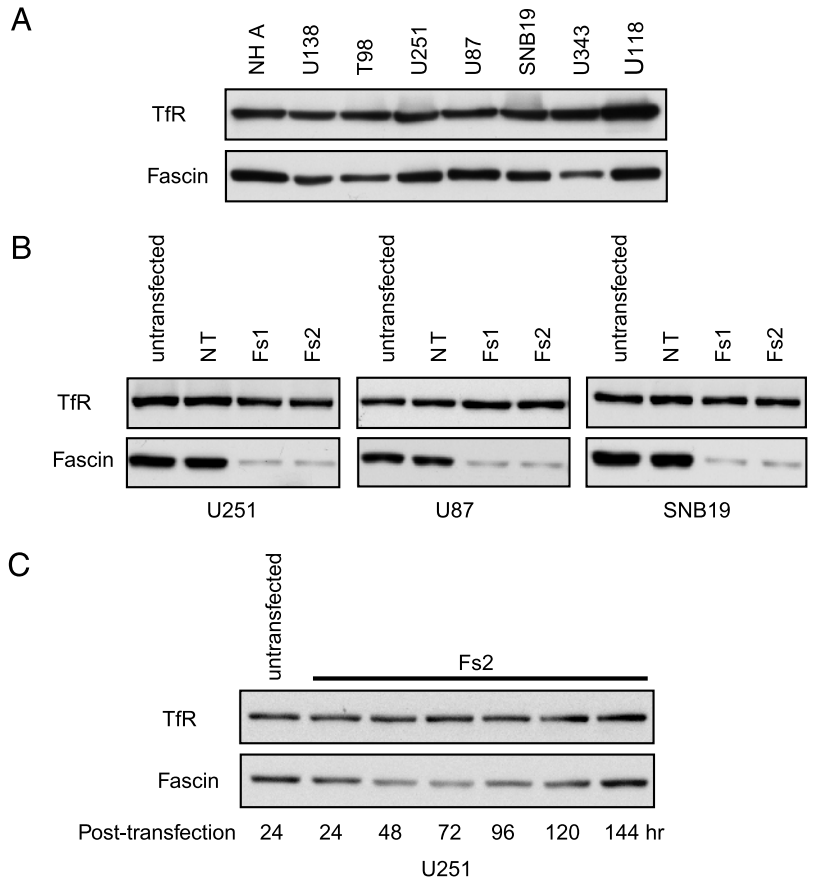

Figure 1. Expression of fascin protein in glioma cell lines and fascin knockdown by siRNA. (A) Western blot analysis of fascin expression in astrocytoma cell lines and normal human astrocytes. (B) Fascin expression following transfection with siRNA for fascin1 in U251, U87, and SNB19 cell lines. (C) Fascin knockdown by siRNA in U251 cells reaches an optimum elimination at 72 hours after transfection. Expression of human transferrin receptor served as a loading control. NHA, normal human astrocytes; NT, nontargeting siRNA; TfR, human transferrin receptor, Fs1 and Fs2, two different fascin1 knockdown sequences used.

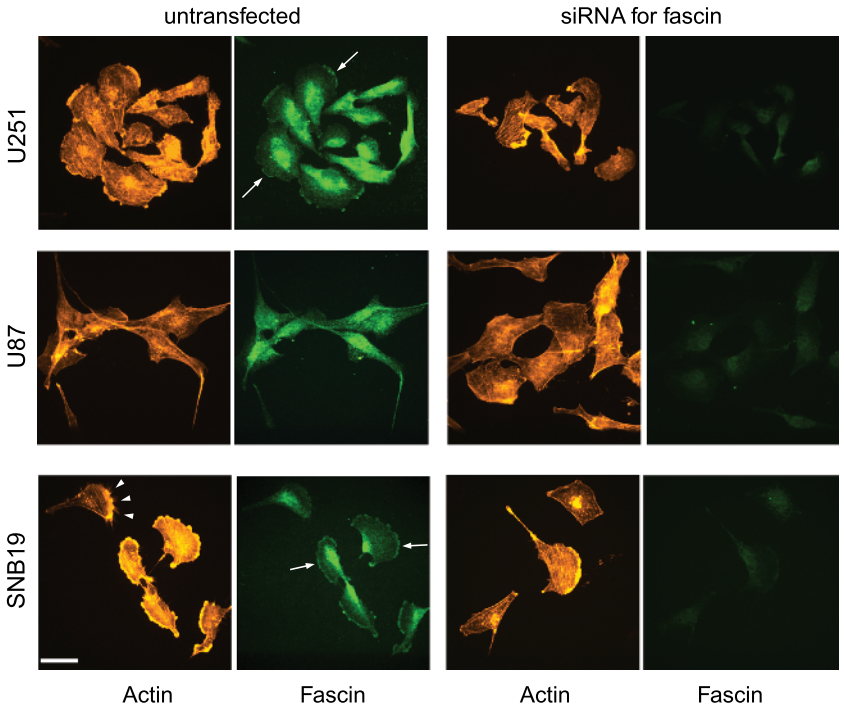

Figure 2. Morphology of glioma cells following fascin siRNA transfection. After siRNA transfection, cells were plated on laminin-precoated coverslips for immunofluorescence. Cells were labeled with Texas Red-X phalloidin for F-actin. Fascin was labeled with anti–fascin antibody followed by Alexa Fluor 488–conjugated anti–mouse antibody. Arrows show staining for fascin at the leading edge in lamellipodia, and arrowheads demonstrate filopodia bundles. Scale bar, 100 μm.

well-organized lamellipodia. Filopodia were also observed at the leading edge especially in SNB19 glioma cells. In contrast to untransfected cells, we observed a decrease in the formation of membrane ruffles in fascin-depleted SNB19 and U251 glioma cells. U87 cells changed cell shape somewhat from typical spindle form of untransfected cells to more polygonal appearances after fascin knockdown. Following fascin knockdown, there was a significant reduction in filopodia formation especially for U87 and SNB19 glioma cells (Figure 3). Filopodia that remained after fascin depletion were of shorter length when compared to controls.

Fascin Elimination Decreases Glioma Cell Adhesion

Given that filopodial formation was significantly inhibited following fascin knockdown, and that filopodia play an important role in cell–ECM adhesion, we predicted that fascin depletion may affect glioma cell adhesion. To determine the effects of fascin knockdown on cell–ECM adhesion, we used different purified ECM macromolecules as substrates for glioma adhesion. Glioma cell lines studied demonstrated different affinities for adhering to ECM macromolecules. In general, glioma cell adhesion was greatest in all cell lines examined when laminin and collagen type IV were used as substrates. Glioma cell adhesion to vitronectin and fibronectin was similar to that of BSA in all three glioma cell lines (Figure 4). The ability of the glioma cell lines to adhere to the different ECM substrates was strongly inhibited by fascin knockdown (Figure 4). These data suggest that, in addition to loss of filopodia by fascin knockdown, glioma cells demonstrate a decreased adhesive capacity when compared to controls. In addition, the data indicate that fascin-dependent adhesion is not attributable to a single ECM macromolecule, as the percentage inhibition of adhesion due to siRNA is similar across all substrates examined.

Fascin Elimination Decreases Migration in Glioma Cells

To determine if fascin plays a role in glioma cell migration, radial migration assays were performed with different purified ECM macromolecules over a 24-hour period. Similar to the results observed in the adhesion study, the migration rate of all three glioma cell lines was enhanced on ECM substrates. After fascin knockdown, all three glioma cell lines showed a significant decrease in migration rate; the migration rate of U251 was decreased on laminin, collagen type IV, and vitronectin by 47.0% ($P < .01$), 24.7% ($P < .01$), and 16.3% ($P < .05$), respectively; U87 migration rate was decreased on laminin and collagen type IV by 47.9% ($P < .01$) and 24.2% ($P < .01$), respectively; the migration rate of SNB19 was decreased on laminin, collagen type IV, vitronectin, and fibronectin by 49.8% ($P < .01$), 39.7% ($P < .01$), 28.2% ($P < .01$), and 28.0% ($P < .01$) by fascin knockdown, respectively (Figure 5).

Fascin Knockdown Decreases Invasion Ability in Glioma Cells In Vitro *and* Ex Vivo

Given that there is a role for fascin in migration and adhesion, we examined the effect of fascin knockdown on glioma cell invasion. The invasiveness of U251, U87 and SNB19 cells was decreased following fascin depletion compared to untransfected cells by 52.2% (mean ± SE, 31.8 ± 3.5 *vs* 66.5 ± 5.9 cells/field; $P < .01$), 40.3% (47.7 ± 3.6 *vs* 79.9 ± 7.1 cells/field; $P < .01$), and 23.8% (47.9 ± 2.9 *vs* 62.9 ± 4.7 cells/field; $P < .01$), respectively. Nontargeting siRNA transfection had no demonstrable effect on the rate of invasion in all three glioma cell lines (Figure 6).

For the *ex vivo* rat brain slice model system, we first demonstrated that fascin expression was suppressed in U251-GFP cells using fascin siRNA (Figure 7*A*). After 72 hours of incubation on the brain slices, the depth of invasion of fascin-depleted U251-GFP cells was decreased (74.2 ± 3.5 μm/72 hours) compared to control cells (94.4 ± 4.4 μm/72 hours; $P < .01$; Figure 7, *B* and *C*).

Discussion

In this study, we have shown that the actin-bundling protein, fascin, is expressed in normal human astrocytes and permanent glioma cell lines. Previously, we demonstrated that fascin is expressed in white matter and cortex of normal brain. Interestingly, fascin expression increased with increasing grade of astrocytoma [35,36]. In the current study, when fascin is downregulated by siRNA, there is an associated decrease in glioma cell adhesion, migration, and *in vitro* invasion. Taken together, these results suggest a role for fascin in glioma invasiveness. Whereas the mechanism by which fascin knockdown reduces glioma invasion is not entirely elucidated, we hypothesize that suppression of fascin may alter the assembly of cytoskeletal proteins, in particular actin microfilaments, in filopodia at the leading edge of motile cells causing a reduction in cell adhesion and migration.

Fascin is principally expressed in neural and mesenchymal derivatives during embryogenesis [45]. In the adult organism, fascin expression is highly tissue- and cell type–specific. For example, fascin is expressed at high levels in the nervous system, especially in neurons, glial cells, and vascular endothelial cells [19–22,46].

Fascin functions in two major forms of actin-based structures: cortical cell protrusions that mediate cell interactions with ECM or other cells and migration; and cytoplasmic microfilamentous bundles that contribute to cell architecture and intracellular movements [13]. Fascin is a key filopodial bundling protein and has a central role in the formation and protrusion of filopodia [13,15]. Vignjevic et al. [15] determined that fascin activity is essential to filopodial dynamics and proposed that fascin imparts rigidity to the forming filopodia to efficiently push the membrane forward.

High-level expression of fascin has been observed in several types of human neoplasms, such as cancer of colon [26,29,33], breast [24], lung [27], kidney [32], ovary [30], cervix [47], and esophagus [28,31]. In node-negative invasive hereditary breast carcinomas, fascin is frequently expressed in BRCA1-associated tumors [48]. Zhang et al. [49] observed that breast cancer metastasis suppressor, *BRMS1*, expression downregulates fascin expression in ovarian carcinoma. Recently, fascin has been regarded as a potential biomarker of early stage cancer [31]. Furthermore, high fascin expression correlated with lymph node or distant metastasis in cancers of colon, kidney, and esophagus, and played a role as an independent marker of poor prognosis [27–29,31–33,50].

Two previous studies have examined the expression of fascin in human gliomas. Peraud et al. [35] reported fascin expression in a panel of human gliomas and observed an increase in fascin expression with increasing tumor grade. Roma and Prayson [36] performed immunohistochemical analysis in gliomas including 90 glioblastomas.

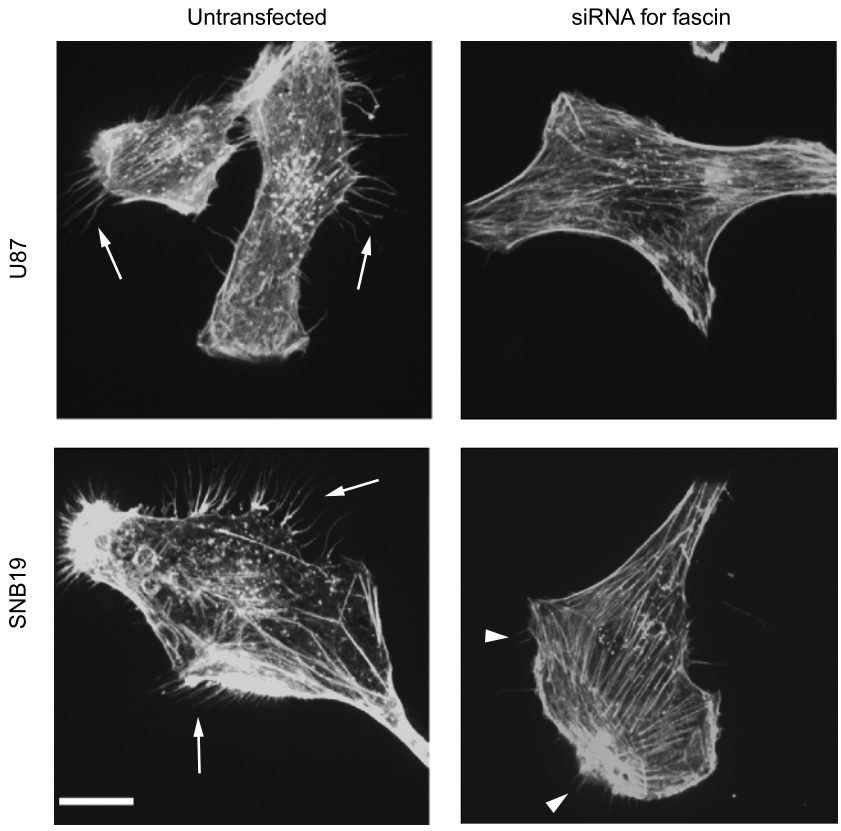

Figure 3. Inhibition of filopodia formation by fascin knockdown. Cells were seeded on laminin-coated coverslips after fascin siRNA transfection. Actin filaments were labeled with Texas Red-X phalloidin. Arrows show filopodial bundles from cell edge in untransfected cells. In contrast to control cells, fascin depleted U87 and SNB19 glioma cells demonstrate reduced number of filopodia. Arrowheads indicate the residual filopodia of SNB19 cell after fascin knockdown. Bar, 25 μm.

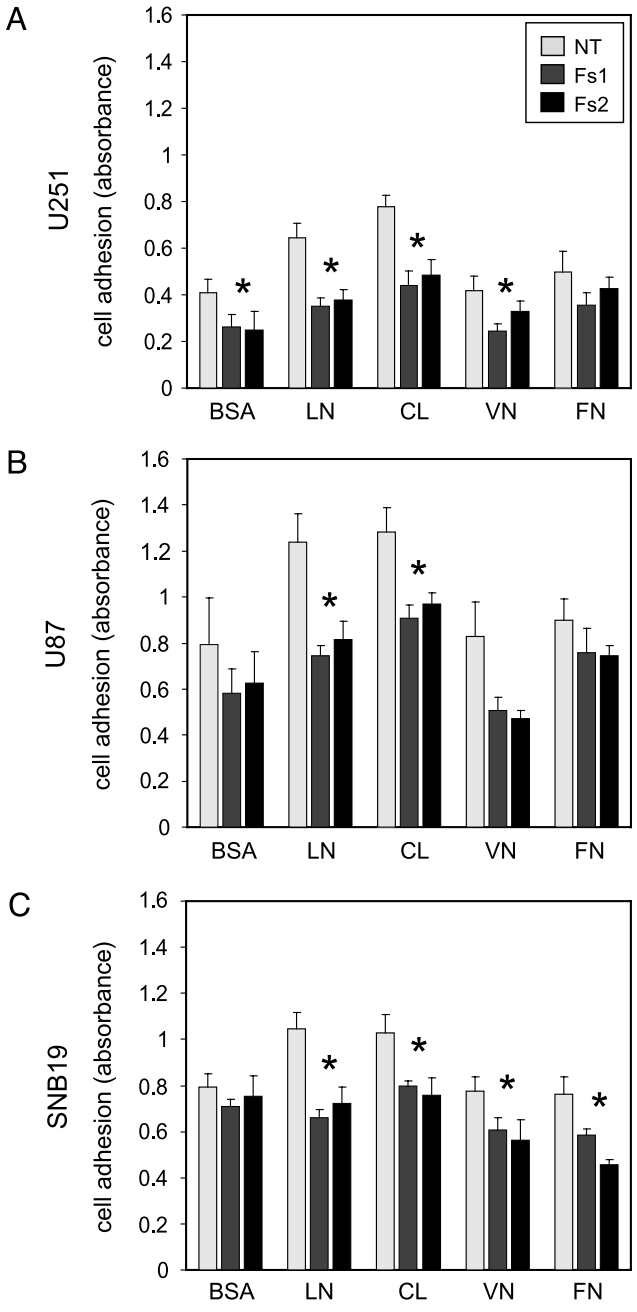

Figure 4. The effects of fascin knockdown on glioma cell adhesion to ECM. (A) U251, (B) U87, and (C) SNB19 cells were plated and allowed to adhere for 3 hours on different ECM substrates at 72 hours after transfection with fascin siRNA. After washing, crystal violet bound to the attached cells were solubilized and the absorbance was measured at 595 nm. Asterisks indicate statistically significant change ($P < .05$) in adhesion after fascin silencing. Columns represent the average optical absorbance of three independent experiments. Bars show SE. LN, laminin; CL, collagen type IV; VN, vitronectin; FN, fibronectin.

They also observed that the higher-grade tumors expressed a greater degree of fascin staining than did the lower-grade tumors. Based on these immunohistochemical data, it has been concluded that fascin expression is correlated with higher-grade malignancy in human glial tumors.

Overexpression of fascin is associated with increased cellular proliferation in different cancers including non–small cell lung adenocarcinoma [27], colon carcinoma [26], and esophageal squamous cell carcinoma [31]. Downregulation of fascin using RNAi resulted in suppression of cell proliferation in esophageal carcinoma cells [34].

Jawhari et al. [26] transfected human colon adenocarcinoma cells with a fascin cDNA and showed that fascin overexpression leads

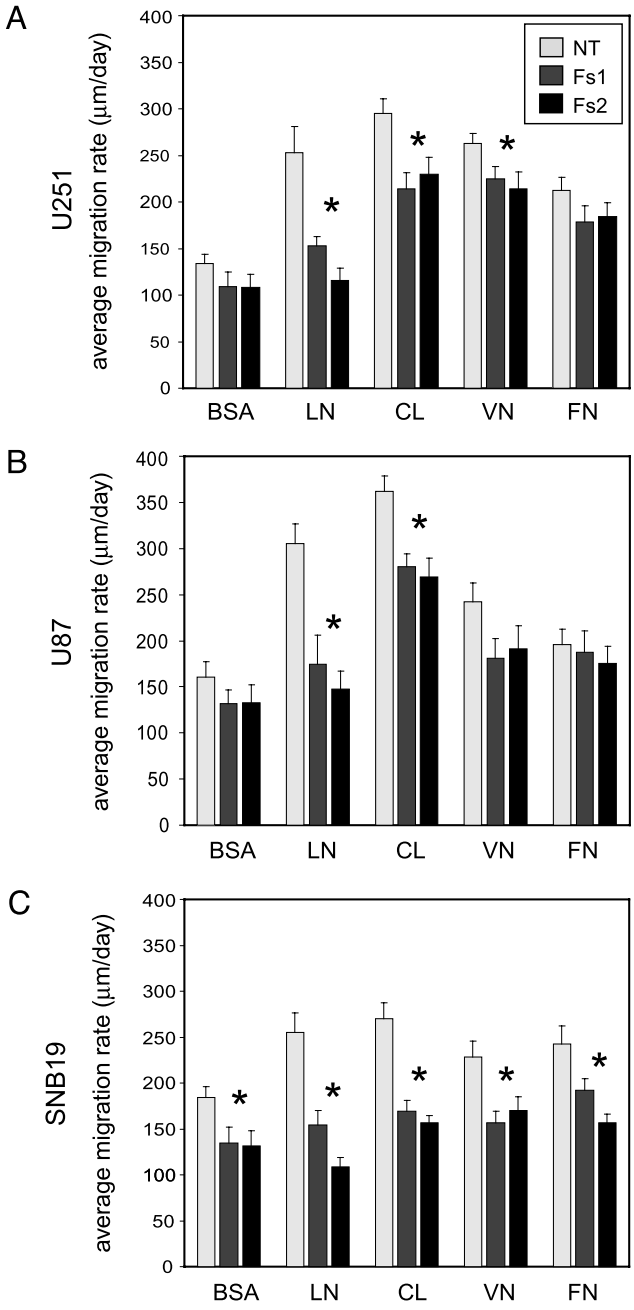

Figure 5. The effects of fascin knockdown on glioma cell migration using microliter-scale radial migration assay. (A) U251, (B) U87, and (C) SNB19 cells were transfected with siRNA and seeded through a cell sedimentation manifold to establish a circular confluent monolayer on substrate-coated well. The cells were allowed to migrate for 24 hours, and photographs were taken before and after migration. Average migration rate was calculated as the change in the diameter of the circle circumscribing the cell population over a 24-hour period. Asterisks indicate statistically significant changes ($P < .05$) in migration rate after fascin silencing. Columns represent the average migration rate of three independent experiments. Bars show SE.

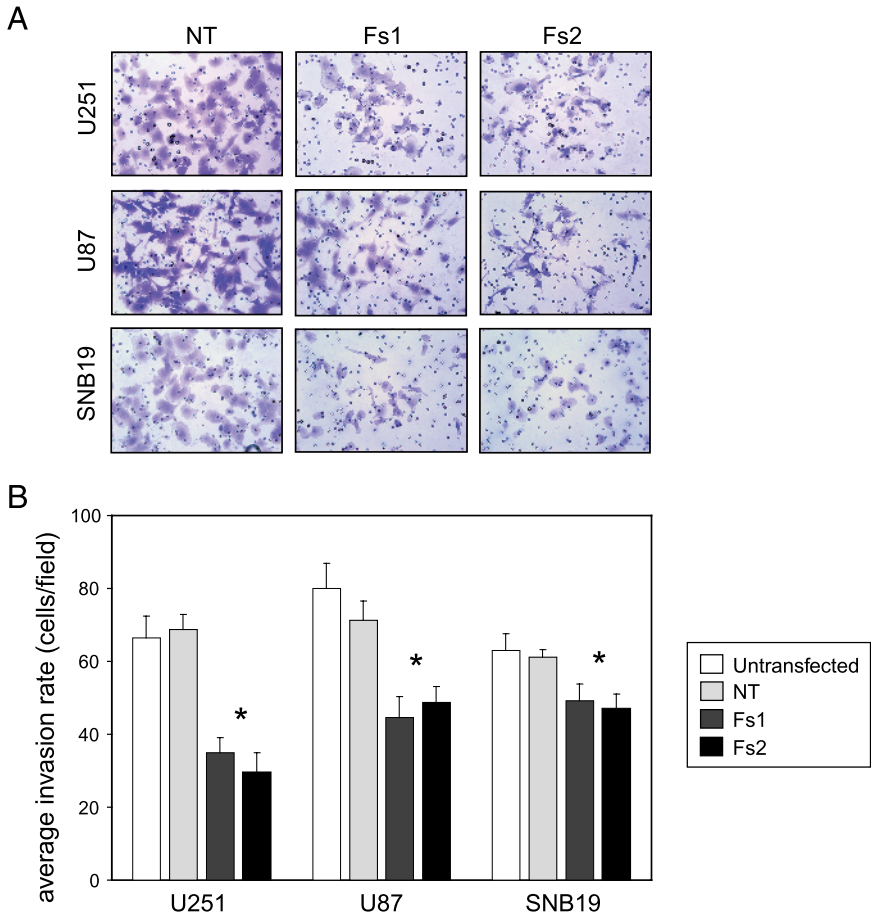

Figure 6. Matrigel invasion assay after fascin elimination. (A) Modified Boyden chamber with Matrigel-precoated membrane filter insert was used to measure *in vitro* invasiveness. After 24 hours of incubation, the cells that migrated through the membrane were stained, and representative fields were photographed. Original magnification, 200×. (B) Invasion was quantified by counting cells in six random fields. The invasion rate of the three cell lines is significantly reduced by fascin depletion. Asterisks indicate statistically significant changes ($P < .01$) after fascin silencing. Columns represent the average of the number of cells per field of at least six fields in three independent experiments. Bars show SE.

to increased dynamic cell protrusions, increased focal contacts formation, increased motility, and increased invasiveness. In contrast, downregulation of fascin using RNAi in esophageal carcinoma cells resulted in significantly reduced cellular motility and invasive properties [28,34]. These data support our observations in human glioma cells.

Previous reports have shown that the fascin–actin interaction is affected by extracellular cues [13,20]. Certain ECM components induce bundling of actin by fascin, whereas others produce inhibitory effects. Adams [21] reported that cells exposed to thrombospondin-1 and tenascin-C activate stable formation of fascin-containing protrusions in fibroblasts, whereas cells that attach to fibronectin or vitronectin show only transient cellular protrusions. It is conceivable that differential phosphorylation of fascin by ECM substrates contributes to these observations. On a molecular basis, the actin-binding activity of fascin is inhibited by phosphorylation of residue Ser-39 by protein kinase Cα (PKCα) [51,52]. Cohan et al. [12] observed that treatment with the PKC activator, 12-*O*-tetradecanoylphorbol-13-acetate, resulted in loss of all actin bundles from growth cones in *Helisoma*. Recently, Vignjevic et al. [15] demonstrated that dephosphorylation of Ser-39 determined filopodial formation in mouse melanoma cells. The constitutively active fascin mutant *S39A* increased the number and length of filopodia, whereas the inactive *S39E* mutant did not.

Several previous reports have demonstrated that fascin silencing is associated with changes in cellular process formation. Stable fascin siRNA transfection of esophageal carcinoma cells led to a decrease in filopodia formation by immunofluorescence analysis [28] and electron microscopy [34]. Vignjevic et al. [15] showed that fascin depletion leads to a reduction in the number of filopodia with the remaining filopodia demonstrating abnormal morphology with waxy and loose actin bundle organization. Our study with human glioma cells corroborates the results of these previous studies.

In attempts to clarify the mechanism by which the elimination of fascin can lead to a reduction in cellular adhesion and migration, Wong et al. [53] showed that ectopic constitutive expression of fascin disrupted the dexamethasone-induced localization of occludin and β-catenin to peripheral cell membranes. Interestingly, Vignjevic et al. [54] showed recently that β-catenin/T cell factor signaling can transactivate the *fascin1* promoter in human colon carcinoma cells. Xie et al. [34] demonstrated that the effect of fascin on cell invasiveness correlated with the activation of matrix metalloproteinase-2 and -9, and confirmed that fascin downregulation is associated with a decrease in β-catenin and c-erbB-2 expression. Grothey et al. [24] have suggested that transcriptional upregulation of fascin in human tumors is dependent on overexpression of c-erbB-2/HER-2. However, the role of c-erbB-2 in malignant gliomas is not clear. In one study, 80% of

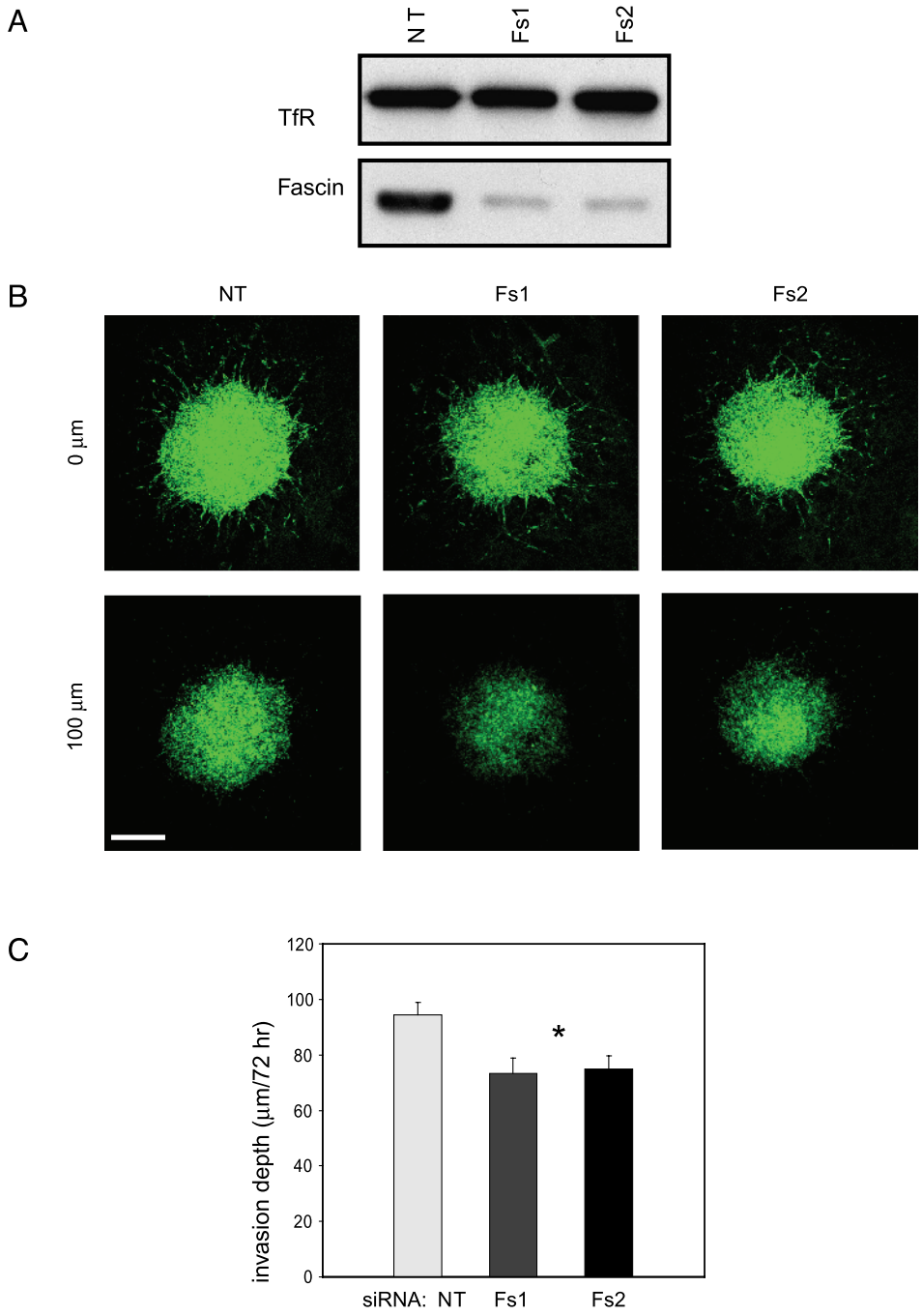

Figure 7. *Ex vivo* invasion assay. (A) Western blot analysis demonstrates fascin knockdown in U251-GFP cells following siRNA transfection. (B) Rat brain slice model system was used to measure *ex vivo* invasiveness. Cells transfected by fascin siRNA were transplanted into the center of putamen on brain slice and allowed to invade for 72 hours. Serial images were taken every 10 µm downward from the top surface to the bottom of the slice with an inverted confocal microscopy, and the area of GFP-stained cells in each section was calculated. Photographs depict the representative fields. Scale bar, 500 µm. (C) The depth of invasion at 72 hours was used to determine the invasiveness of the glioma cells. The depth of invasion of fascin depleted cells decreased by 21.4% ($P < .01$) compared to control cells. The mean value was obtained from three experiments. Bars show SE.

glioblastoma cells showed expression of c-erbB-2/HER-2 [55], whereas in another study overexpression of c-erbB-2/HER-2 was detected in only 15% of glioblastoma tumor specimens [56].

In summary, fascin depletion in glioma cells results in decreased filopodial formation and decreased migration suggesting that fascin plays a key role in glioma invasiveness. The molecular mechanisms by which fascin interacts with actin and other cytoskeletal proteins to alter glioma cell motility, the use of a stable fascin knockdown system *in vivo*, and the development of pharmacological inhibitors of fascin will be instrumental in furthering our understanding of the role of fascin dynamics in human malignant gliomas.

References

[1] Burger PC, Vogel FS, Green SB, and Strike TA (1985). Glioblastoma multiforme and anaplastic astrocytoma. Pathologic criteria and prognostic implications. *Cancer* **56** (5), 1106–1111.

[2] Stupp R, Hegi ME, Gilbert MR, and Chakravarti A (2007). Chemoradiotherapy in malignant glioma: standard of care and future directions. *J Clin Oncol* **25** (26), 4127–4136.

[3] Soffietti R, Leoncini B, and Ruda R (2007). New developments in the treatment of malignant gliomas. *Expert Rev Neurother* **7** (10), 1313–1326.

[4] Goffman TE, Dachowski LJ, Bobo H, Oldfield EH, Steinberg SM, Cook J, Mitchell JB, Katz D, Smith R, and Glatstein E (1992). Long-term follow-up on National Cancer Institute Phase I/II study of glioblastoma multiforme treated with iododeoxyuridine and hyperfractionated irradiation. *J Clin Oncol* **10** (2), 264–268.

[5] Senger D, Cairncross JG, and Forsyth PA (2003). Long-term survivors of glioblastoma: statistical aberration or important unrecognized molecular subtype? *Cancer J* **9** (3), 214–221.

[6] Giese A, Rief MD, Loo MA, and Berens ME (1994). Determinants of human astrocytoma migration. *Cancer Res* **54** (14), 3897–3904.

[7] Giese A, Bjerkvig R, Berens ME, and Westphal M (2003). Cost of migration: invasion of malignant gliomas and implications for treatment. *J Clin Oncol* **21** (8), 1624–1636.

[8] Demuth T and Berens ME (2004). Molecular mechanisms of glioma cell migration and invasion. *J Neurooncol* **70** (2), 217–228.

[9] Lauffenburger DA and Horwitz AF (1996). Cell migration: a physically integrated molecular process. *Cell* **84** (3), 359–369.

[10] Adams JC (2004). Roles of fascin in cell adhesion and motility. *Curr Opin Cell Biol* **16** (5), 590–596.

[11] Bartles JR (2000). Parallel actin bundles and their multiple actin-bundling proteins. *Curr Opin Cell Biol* **12** (1), 72–78.

[12] Cohan CS, Welnhofer EA, Zhao L, Matsumura F, and Yamashiro S (2001). Role of the actin bundling protein fascin in growth cone morphogenesis: localization in filopodia and lamellipodia. *Cell Motil Cytoskeleton* **48** (2), 109–120.

[13] Kureishy N, Sapountzi V, Prag S, Anilkumar N, and Adams JC (2002). Fascins, and their roles in cell structure and function. *Bioessays* **24** (4), 350–361.

[14] Salhia B, Rutten F, Nakada M, Beaudry C, Berens M, Kwan A, and Rutka JT (2005). Inhibition of Rho-kinase affects astrocytoma morphology, motility, and invasion through activation of Rac1. *Cancer Res* **65** (19), 8792–8800.

[15] Vignjevic D, Kojima S, Aratyn Y, Danciu O, Svitkina T, and Borisy GG (2006). Role of fascin in filopodial protrusion. *J Cell Biol* **174** (6), 863–875.

[16] Kane RE (1975). Preparation and purification of polymerized actin from sea urchin egg extracts. *J Cell Biol* **66** (2), 305–315.

[17] Cant K, Knowles BA, Mooseker MS, and Cooley L (1994). *Drosophila singed*, a fascin homolog, is required for actin bundle formation during oogenesis and bristle extension. *J Cell Biol* **125** (2), 369–380.

[18] Mosialos G, Yamashiro S, Baughman RW, Matsudaira P, Vara L, Matsumura F, Kieff E, and Birkenbach M (1994). Epstein-Barr virus infection induces expression in B lymphocytes of a novel gene encoding an evolutionarily conserved 55-kilodalton actin-bundling protein. *J Virol* **68** (11), 7320–7328.

[19] Edwards RA and Bryan J (1995). Fascins, a family of actin bundling proteins. *Cell Motil Cytoskeleton* **32** (1), 1–9.

[20] Adams JC (1995). Formation of stable microspikes containing actin and the 55 kDa actin bundling protein, fascin, is a consequence of cell adhesion to thrombospondin-1: implications for the anti-adhesive activities of thrombospondin-1. *J Cell Sci* **108** (Pt 5), 1977–1990.

[21] Adams JC (1997). Characterization of cell–matrix adhesion requirements for the formation of fascin microspikes. *Mol Biol Cell* **8** (11), 2345–2363.

[22] Adams JC, Kureishy N, and Taylor AL (2001). A role for syndecan-1 in coupling fascin spike formation by thrombospondin-1. *J Cell Biol* **152** (6), 1169–1182.

[23] Yamashiro-Matsumura S and Matsumura F (1986). Intracellular localization of the 55-kD actin-bundling protein in cultured cells: spatial relationships with actin, alpha-actinin, tropomyosin, and fimbrin. *J Cell Biol* **103** (2), 631–640.

[24] Grothey A, Hashizume R, Ji H, Tubb BE, Patrick CW Jr, Yu D, Mooney EE, and McCrea PD (2000). C-erbB-2/HER-2 upregulates fascin, an actin-bundling protein associated with cell motility, in human breast cancer cell lines. *Oncogene* **19** (42), 4864–4875.

[25] Grothey A, Hashizume R, Sahin AA, and McCrea PD (2000). Fascin, an actin-bundling protein associated with cell motility, is upregulated in hormone receptor negative breast cancer. *Br J Cancer* **83** (7), 870–873.

[26] Jawhari AU, Buda A, Jenkins M, Shehzad K, Sarraf C, Noda M, Farthing MJ, Pignatelli M, and Adams JC (2003). Fascin, an actin-bundling protein, modulates colonic epithelial cell invasiveness and differentiation *in vitro*. *Am J Pathol* **162** (1), 69–80.

[27] Pelosi G, Pastorino U, Pasini F, Maissoneuve P, Fraggetta F, Iannucci A, Sonzogni A, De Manzoni G, Terzi A, Durante E, et al. (2003). Independent prognostic value of fascin immunoreactivity in stage I nonsmall cell lung cancer. *Br J Cancer* **88** (4), 537–547.

[28] Hashimoto Y, Ito T, Inoue H, Okumura T, Tanaka E, Tsunoda S, Higashiyama M, Watanabe G, Imamura M, and Shimada Y (2005). Prognostic significance of fascin overexpression in human esophageal squamous cell carcinoma. *Clin Cancer Res* **11** (7), 2597–2605.

[29] Hashimoto Y, Skacel M, Lavery IC, Mukherjee AL, Casey G, and Adams JC (2006). Prognostic significance of fascin expression in advanced colorectal cancer: an immunohistochemical study of colorectal adenomas and adenocarcinomas. *BMC Cancer* **6**, 241.

[30] Kabukcuoglu S, Ozalp SS, Oner U, Bildirici K, Yalcin OT, Oge T, and Colak E (2006). Actin bundling protein fascin expression in ovarian neoplasms: comparison of histopathologic features of tumors obtained by the first and secondary cytoreduction surgeries. *Eur J Gynaecol Oncol* **27** (2), 123–128.

[31] Zhang H, Xu L, Xiao D, Xie J, Zeng H, Cai W, Niu Y, Yang Z, Shen Z, and Li E (2006). Fascin is a potential biomarker for early-stage oesophageal squamous cell carcinoma. *J Clin Pathol* **59** (9), 958–964.

[32] Zigeuner R, Droschl N, Tauber V, Rehak P, and Langner C (2006). Biologic significance of fascin expression in clear cell renal cell carcinoma: systematic analysis of primary and metastatic tumor tissues using a tissue microarray technique. *Urology* **68** (3), 518–522.

[33] Puppa G, Maisonneuve P, Sonzogni A, Masullo M, Chiappa A, Valerio M, Zampino MG, Franceschetti I, Capelli P, Chilosi M, et al. (2007). Independent prognostic value of fascin immunoreactivity in stage III–IV colonic adenocarcinoma. *Br J Cancer* **96** (7), 1118–1126.

[34] Xie JJ, Xu LY, Zhang HH, Cai WJ, Mai RQ, Xie YM, Yang ZM, Niu YD, Shen ZY, and Li EM (2005). Role of fascin in the proliferation and invasiveness of esophageal carcinoma cells. *Biochem Biophys Res Commun* **337** (1), 355–362.

[35] Peraud A, Mondal S, Hawkins C, Mastronardi M, Bailey K, and Rutka JT (2003). Expression of fascin, an actin-bundling protein, in astrocytomas of varying grades. *Brain Tumor Pathol* **20** (2), 53–58.

[36] Roma AA and Prayson RA (2005). Fascin expression in 90 patients with glioblastoma multiforme. *Ann Diagn Pathol* **9** (6), 307–311.

[37] Elbashir SM, Harborth J, Lendeckel W, Yalcin A, Weber K, and Tuschl T (2001). Duplexes of 21-nucleotide RNAs mediate RNA interference in cultured mammalian cells. *Nature* **411** (6836), 494–498.

[38] Sriramarao P, Mendler M, and Bourdon MA (1993). Endothelial cell attachment and spreading on human tenascin is mediated by alpha 2 beta 1 and alpha v beta 3 integrins. *J Cell Sci* **105** (Pt 4), 1001–1012.

[39] Berens ME, Rief MD, Loo MA, and Giese A (1994). The role of extracellular matrix in human astrocytoma migration and proliferation studied in a microliter scale assay. *Clin Exp Metastasis* **12** (6), 405–415.

[40] Valster A, Tran NL, Nakada M, Berens ME, Chan AY, and Symons M (2005). Cell migration and invasion assays. *Methods* **37** (2), 208–215.

[41] Ohnishi T, Matsumura H, Izumoto S, Hiraga S, and Hayakawa T (1998). A novel model of glioma cell invasion using organotypic brain slice culture. *Cancer Res* **58** (14), 2935–2940.

[42] Jung S, Ackerley C, Ivanchuk S, Mondal S, Becker LE, and Rutka JT (2001). Tracking the invasiveness of human astrocytoma cells by using green fluorescent protein in an organotypical brain slice model. *J Neurosurg* **94** (1), 80–89.

[43] Nakada M, Niska JA, Miyamori H, McDonough WS, Wu J, Sato H, and Berens ME (2004). The phosphorylation of EphB2 receptor regulates migration and invasion of human glioma cells. *Cancer Res* **64** (9), 3179–3185.

[44] Rutka JT, Muller M, Hubbard SL, Forsdike J, Dirks PB, Jung S, Tsugu A, Ivanchuk S, Costello P, Mondal S, et al. (1999). Astrocytoma adhesion to extracellular matrix: functional significance of integrin and focal adhesion kinase expression. *J Neuropathol Exp Neurol* **58** (2), 198–209.

[45] De Arcangelis A, Georges-Labouesse E, and Adams JC (2004). Expression of *fascin-1*, the gene encoding the actin-bundling protein fascin-1, during mouse embryogenesis. *Gene Expr Patterns* **4** (6), 637–643.

[46] Edwards RA, Herrera-Sosa H, Otto J, and Bryan J (1995). Cloning and expression of a murine fascin homolog from mouse brain. *J Biol Chem* **270** (18), 10764–10770.

[47] Kabukcuoglu S, Ozalp SS, Oner U, Acikalin MF, Yalcin OT, and Colak E (2005). Fascin, an actin-bundling protein expression in cervical neoplasms. *Eur J Gynaecol Oncol* **26** (6), 636–641.

[48] Rodriguez-Pinilla SM, Sarrio D, Honrado E, Hardisson D, Calero F, Benitez J, and Palacios J (2006). Prognostic significance of basal-like phenotype and fascin

expression in node-negative invasive breast carcinomas. *Clin Cancer Res* **12** (5), 1533–1539.

[49] Zhang S, Lin QD, and Di W (2006). Suppression of human ovarian carcinoma metastasis by the metastasis-suppressor gene, *BRMS1*. *Int J Gynecol Cancer* **16** (2), 522–531.

[50] Chen SF, Yang SF, Li JW, Nieh PC, Lin SY, Fu E, Bai CY, Jin JS, Lin CY, and Nieh S (2007). Expression of fascin in oral and oropharyngeal squamous cell carcinomas has prognostic significance—a tissue microarray study of 129 cases. *Histopathology* **51** (2), 173–183.

[51] Ono S, Yamakita Y, Yamashiro S, Matsudaira PT, Gnarra JR, Obinata T, and Matsumura F (1997). Identification of an actin binding region and a protein kinase C phosphorylation site on human fascin. *J Biol Chem* **272** (4), 2527–2533.

[52] Adams JC, Clelland JD, Collett GD, Matsumura F, Yamashiro S, and Zhang L (1999). Cell–matrix adhesions differentially regulate fascin phosphorylation. *Mol Biol Cell* **10** (12), 4177–4190.

[53] Wong V, Ching D, McCrea PD, and Firestone GL (1999). Glucocorticoid down-regulation of fascin protein expression is required for the steroid-induced formation of tight junctions and cell–cell interactions in rat mammary epithelial tumor cells. *J Biol Chem* **274** (9), 5443–5453.

[54] Vignjevic D, Schoumacher M, Gavert N, Janssen KP, Jih G, Lae M, Louvard D, Ben-Ze'ev A, and Robine S (2007). Fascin, a novel target of beta-catenin–TCF signaling, is expressed at the invasive front of human colon cancer. *Cancer Res* **67** (14), 6844–6853.

[55] Liu G, Ying H, Zeng G, Wheeler CJ, Black KL, and Yu JS (2004). HER-2, gp100, and MAGE-1 are expressed in human glioblastoma and recognized by cytotoxic T cells. *Cancer Res* **64** (14), 4980–4986.

[56] Koka V, Potti A, Forseen SE, Pervez H, Fraiman GN, Koch M, and Levitt R (2003). Role of Her-2/*neu* overexpression and clinical determinants of early mortality in glioblastoma multiforme. *Am J Clin Oncol* **26** (4), 332–335.